Atomic oxygen and hydroxyl density measurements in an atmospheric pressure RF-plasma with water admixtures using UV and synchrotron VUV absorption spectroscopy

S. Schröter[1], M. Foucher[2], K. Niemi[1], J. Dedrick[1], N. de Oliveira[3], D. Joyeux[3], L. Nahon[3], E. Wagenaars[1], T. Gans[1], J.P. Booth[2] and D. O'Connell[1]

[1] *York Plasma Institute, Department of Physics, University of York, Heslington, York YO10 5DQ, U.K.*
[2]*Laboratoire de Physique des Plasmas, Ecole Polytechnique, 91128 Palaiseau Cedex, France*
[3]*Synchrotron Soleil, l'Orme des Merisiers, St. Aubin P.O. Box 48, 91192 Gif sur Yvette Cedex, France*

Abstract: Absolute O and OH ground state densities were measured in a He rf-plasma (13.56 MHz driving frequency) with water admixtures. For this, high resolution synchrotron VUV and broadband UV absorption spectroscopy was used. Detected absolute O and OH densities were in the order of 10^{19} and 10^{20} m^{-3}, respectively. The densities of both species were found to increase towards higher water admixtures.

Keywords: reactive oxygen species, absorption spectroscopy, water, hydroxyl radical

1. Motivation

The application of low temperature atmospheric pressure plasmas, for many technological applications, is an emerging field of research. Atmospheric pressure plasmas are known to be a source of highly reactive oxygen species (ROS), which play an important role in many medical therapeutics e.g. cancer treatment [1]. In particular the determination of reactive atomic oxygen (O) and hydroxyl radicals (OH) is of great interest, since they serve as precursors for long lived species like hydrogen peroxide or ozone. O and OH can be created when the plasma is in contact with oxygen molecules (O_2) or water (H_2O), both of which are naturally present in ambient air, or can be actively admixed to the gas flow feeding the plasma. Regulation of the produced reactive species by controlling these admixtures is desired.

However, especially at atmospheric pressure, the detection of the discussed species is challenging due to fast collision rates of the particles and their high reactivity. Different approaches have been used in the past in order to determine O and OH densities, mostly applying conventional (Two-photon Absorption) Laser-Induced Fluorescence ((TA)LIF) with nanosecond resolution [2-4]. However, if the lifetimes of the excited states cannot be resolved, this technique requires the knowledge of experimentally determined quenching coefficients for collisions with all possible reactions partners as well as the composition of the gas. This becomes especially challenging when examining plasmas with complex gas mixtures.

In this work, broadband absorption spectroscopy (BBAS) is used in order to determine absolute values of $O(^3P)$ and $OH(X)$ densities, dependent on the water content in the plasma. This technique is independent of quenching and does not require additional calibration in order to obtain absolute densities [5]. The wavelength regime for the observable transitions in O and OH lies in the (vacuum) UV and is therefore challenging for diagnostics. For the measurements presented in this work, we used a very stable broadband lamp (OH) and synchrotron radiation (O).

2. Experiment

The plasma source used for the investigations presented here is shown in fig. 1. The plasma is ignited between two plane-parallel stainless steel electrodes with an electrode area of (30 x 8.6) mm^2 and distance of 1 mm. It is confined in the channel by using two MgF_2 windows, which allow optical access far into the UV. Therefore, the discharge is a modified version of the µ-APPJ as described by *Schulz-von der Gathen* [6], but with a larger depth in order to provide a longer absorption length l = 8.6 mm, and as a closed sealed system which enables measurements in high-vacuum environments. A similar source was described earlier by *Niemi et al.* [7]. The operation frequency of the source is 13.56 MHz. Due to the fact that two different power generators were used during the investigations of $O(^3P)$ and $OH(X)$ densities, the plasma was operated with a power close to the arcing point in pure helium as a reference point.

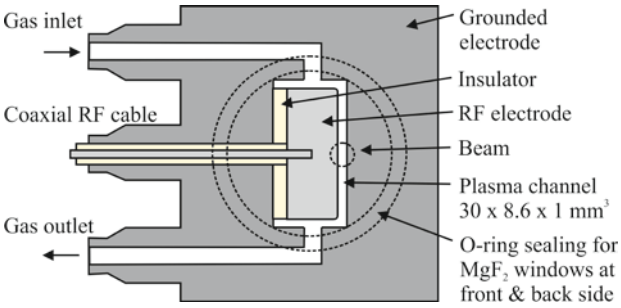

Fig. 1. Plasma source used for the absorption measurements. The absorption length used for the calculations is l = 8.6 mm.

Water was actively admixed to the dry helium gas flow (5 slm in total) by using a system of two mass flow controllers (MFCs), with one MFC regulating helium going through a homemade bubbler. The total amount of water in the plasma can be controlled by mixing the wet and dry helium.

Absorption measurements were carried out in the centre of the discharge gap, as indicated in fig. 1. The light beam was bigger than the discharge gap, therefore, all densities presented here are volume averaged values. The measurements for each species were carried out in two different experimental setups, which will be described in the following paragraphs.

The measurements of absolute O(^{3}P) densities were carried out at the DESIRS (Dichroïsme Et Spectroscopie par Interaction avec le Rayonnement Synchrotron) beamline at the SOLEIL synchrotron [8], using an ultra-high resolution Fourier-transform spectrometer [9] with a resolving power up to $\delta\lambda/\lambda = 1\cdot10^6$. Using this spectrometer enables the spectrally resolved measurements of the Doppler and pressure broadened $2p^4\,{}^3P_2 \rightarrow 3s\,{}^3S^*_1$ transmission line at 130.22 nm [10], which results in a final line shape of a Voigt profile. Additionally, the measured spectra are convolved with the instrumental function of the spectrometer, which is a sinc function $\phi_I = \sin(\pi\Delta\tilde{\nu})/\pi\Delta\tilde{\nu}$, where $\tilde{\nu}$ is the wavenumber. After the deconvolution of the two different line shapes, transmission spectra can be obtained, as shown in fig. 2. The procedure to obtain absolute O(^{3}P) densities was previously described by *Niemi et al.* [7] and will not be described here.

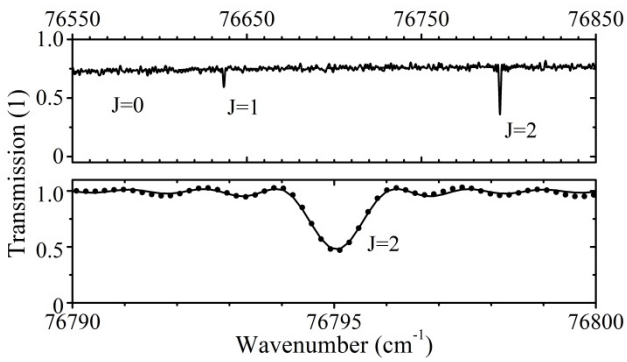

Fig. 2. Typical transmission spectrum of the O ($2p^4\,{}^3P_J \rightarrow 3s\,{}^3S^*_1$) transition for J = 0-2 (top) and J = 2 (bottom). The latter was used for the determination of absolute O(^{3}P) densities as described in [7]. The plasma was operated with a generator power of 9 W and 5 slm total He flow, whereas 400 sccm went through the bubbler. The corresponding O(^{3}P) density is $4.0\cdot10^{19}$ m^{-3}.

For the measurement of absolute OH(X) densities, light from a broadband light source (Energetiq LDLS EQ-99CAL) was focused into the plasma and after that onto the entrance slit of a spectrograph (IsoPlane SCT320, Princeton Instruments), using a set of parabolic mirrors. The light gets partially absorbed when matching a resonance following Beer-Lambert law:

$$T(\lambda) = \frac{I(\lambda)}{I_0(\lambda)} = e^{-A(\lambda)} \qquad (1)$$

$$A(\lambda) = \sum_{J'J''} \sigma^0_{J'J''}\, \phi(\lambda_0 - \lambda_{J'J''}) n_{J''}\, l \qquad (2)$$

where λ is the wavelength, T the transmission, I the measured intensity with and I_0 without absorbing medium and A the absorbance. A depends on the line shape $\phi(\lambda_0 - \lambda_{J'J''})$, the density of the lower energetic state $n_{J''}$, the absorption length l and the cross sections for each rotational transition $\sigma^0_{J'J''} = \frac{g_{J'}}{g_{J''}} \frac{h\lambda^4_{J'J''}}{8\pi c} A_{J'J''}$ where h is Planck's constant, c the speed of light, g the statistical weight and $A_{J'J''}$ the Einstein coefficient for spontaneous emission. For the evaluation of our data, we calculated relative Einstein coefficients for twelve branches according to *Earls* [11] and normalised to an experimental value for the $P_1(2)$ line given by *German* [12].

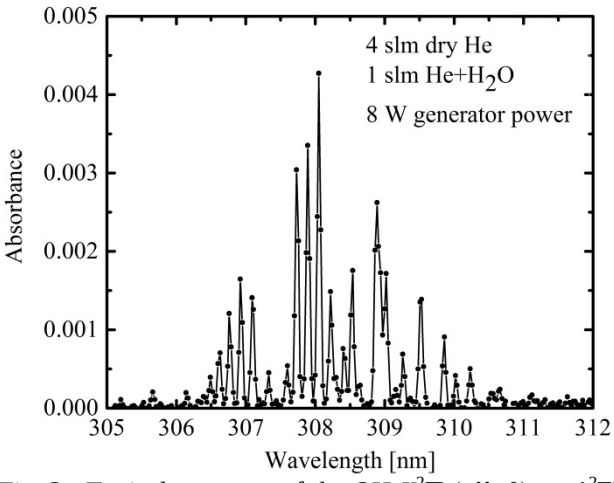

Fig. 3. Typical spectrum of the OH $X^2\Pi$ (υ''=0) → $A^2\Sigma^+$ (υ' = 0) transition. Dots indicate measured points. The total He flow is 5 slm of which 1 slm goes through the bubbler. The generator power is 8 W and the corresponding OH density $n_{OH} = 2.64\cdot10^{20}$ m^{-3}.

Fig. 3 shows a typical absorbance spectrum for the OH $X^2\Pi$ (υ''=0) → $A^2\Sigma^+$ (υ'=0) transition. One can see a relatively strong broadening of the lines, which mainly results from the limited resolution of the spectrograph and the related instrumental function ϕ_I, which is convolved with the transmission. Assuming a Gaussian line profile for ϕ_I, the full width at half maximum and therefore the spectral resolution is 55 pm for our measured spectra. This broadening is a lot larger than that occurring due to Doppler $\Delta\lambda_D$ and pressure broadening $\Delta\lambda_P$ of the lines:

$$\Delta\lambda_D = \frac{\lambda_0}{c}\sqrt{\frac{8k_B T \ln(2)}{m}} \qquad (3)$$

with k_B as the Boltzmann constant, T the gas temperature and m the mass of the OH molecule. Using T = 300 K, $\Delta\lambda_D$ = 0.93 pm. An experimental value for $\Delta\lambda_P$ (for T = 300 K, in He at atmospheric pressure) can be obtained from *Kasyutich* [13] as 0.66 pm.

From the measured absorbance spectra, absolute $n_{J''}$ densities can be retrieved from eq. (2). Absolute ground state densities n can be calculated using a Boltzmann population distribution:

$$\frac{n_{J''}}{n} = \frac{g_{J''} e^{-\frac{hcF_{J''}}{k_B T}}}{\sum_{J''} g_{J''} e^{-\frac{hcF_{J''}}{k_B T}}} \quad (4)$$

where $F_{J''}$ is the rotational term energy in units of cm^{-1}.

3. Results and discussion

Fig. 4 shows the absolute O(^{3}P) and OH(X) densities obtained by the two BBAS techniques described previously, dependent on the water content in the plasma. Water admixtures are indicated as absolute helium gas flow through the bubbler (bottom x-axis) and as percentage of the total flow (top x-axis) calculated using [14]

$$p_v = 6.1094 \cdot 10^{-3} e^{-\frac{17.625T}{243.04\,°C+T}} \quad (5)$$

$$F_{H_2O} = F_{He} \frac{p_v}{p_a - p_v} \quad (6)$$

where p_v is the water vapour pressure in bar, p_a the atmospheric pressure in bar, T the temperature in °C, and F_{He} and F_{H2O} the gas flow of the dry helium that goes through the bubbler, and of the water vapour only, respectively.

Measured OH densities increase non-linearly from 1.7 to $3.3 \cdot 10^{20}$ m^{-3} in the investigated range of water admixtures ((0.25 – 3) slm of the total helium flow goes through the bubbler). According to recent simulation results by *Ding and Lieberman* [15] in a similar system to the one investigated here (atmospheric rf He plasma with 0.1% water admixture, 0.5 mm electrode gap), the main reaction pathways for the creation of OH in a He/H_2O plasma is dissociation of H_2O by collisions with atomic oxygen metastables (O(^{1}D)) and cluster formation induced by Penning ionisation of water by helium metastables (He_m, combined metastable state of 2^1S and 2^3S):

$$O(^1D) + H_2O \rightarrow 2\,OH \quad (7)$$

$$He_m + 6\,H_2O \rightarrow H_{11}O_5^+ + OH + He + e^- \quad (8)$$

Eq. (8) is a multistep process [15]. The authors suggest that about 40% of the total production of OH under their conditions is a result of these two pathways. Therefore, a large part of the OH production is directly related to the H_2O admixture, so that a higher admixture leads to a higher OH density in the plasma.

However, at higher water admixtures, more energy can be coupled into molecular energy states. This means that the effectiveness of the two main production channels for OH mentioned earlier decreases, since they directly rely on electron impact excitation of He to form He_m and electron impact dissociation of O_2 to form O(^{1}D) [15], and therefore on the electron energy:

$$e^- + O_2 \rightarrow O + O(^1D) + e^-. \quad (9)$$

Because of this, the slope in the OH density shown in fig. 4 is less steep at higher water admixtures. Further points at higher water admixtures could not be taken, because the plasma extinguishes.

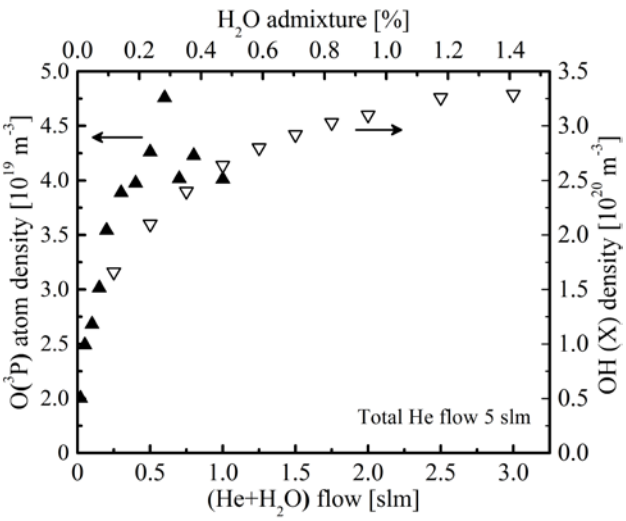

Fig. 4. Absolute O and OH densities depending on the water content in the plasma. The bottom x-axis shows the amount of helium going through the bubbler at an overall constant gas flow of 5 slm. The top x-axis shows the corresponding percentages of water calculated using eq. (5) [14] and (6) assuming complete saturation and T = 20 °C.

Measured O densities are in general about a factor of 4 to 6 lower compared to the OH density. The main production channels according to [15] are electron impact dissociation of O_2 as indicated in eq. (9) and the deexcitation of O(^{1}D) by collisions with He atoms. These reactions are only indirectly related to the H_2O admixture, which makes the interpretation of the results more difficult.

At low water admixtures (< 0.2%), the amount of O increases with increasing water content. This indicates that O_2 is produced from species generated indirectly from H_2O like HO_2. At higher water admixtures around 0.3%, the measured O densities seem to level off, which indicates either a decrease in O_2 production or a competitive process which increases the O_2 destruction. In the former case (as in the case of the OH), a higher

molecular admixture leads to a lower effectiveness of the plasma, which would lead to a lower O_2 production. For future measurements it is planned to quantify O densities at even higher admixtures to see if the density stays on the same level or decreases, as it was seen previously in the case of the variation of the molecular oxygen admixture to the plasma in the absence of H_2O [16].

4. Conclusions and Outlook

Absolute O and OH densities were determined using two different BBAS techniques. In our measurement range, OH increased continuously with increasing water admixture up to about 1.4% due to direct OH production from H_2O. At higher water admixtures, the plasma extinguishes. Measured densities were in the range of (1.7 – 3.3)$\cdot 10^{20}$ m^{-3}. O was found to increase up to approximately 0.2% water admixture and after that levelled off until about 0.5%, which was the end of our investigated measurement range. The interpretation of the data is challenging, since the O production is not directly related to the H_2O admixture. Absolute O densities are (2.0 – 4.8)$\cdot 10^{19}$ m^{-3}.

Future measurements could include an extension of the investigated range in the case of O, to see if there is a decrease in O as it was measured previously in a He-O_2 plasma [16]. Additionally, measurements using absorption spectroscopy could be widened to measure other species of interest such as O_3.

5. Acknowledgements

This work was performed within the LABEX Plas@par project and received financial state aid, managed by the Agence National de la Recherche as part of the programme “Investissements d’avenir” (ANR-11-IDEX-0004-02). Financial support was also received from the UK EPSRC (EP/K018388/1 & EP/H003797/1) and the York-Paris Low Temperature Plasma Collaborative Research Centre.

6. References

[1] D. Graves. *J. Phys. D: Appl. Phys.*, **45**, 263001 (2012)
[2] K. Niemi, V. Schulz-von der Gathen, H. F. Döbele. *Plasma Sources Sci. Technol.*, **14**, 375-386 (2005)
[3] S. Reuter, J. Winter, A. Schmidt-Bleker, D. Schroeder, H. Lange, N. Knake, V. Schulz-von der Gathen, K.-D. Weltmann. *Plasma Sources Sci. Technol.*, **21**, 024005 (2012)
[4] T. Verreycken, R. Mensink, R. van der Horst, N. Sadeghi, P. J. Bruggeman. *Plasma Sources Sci. Technol.*, **22**, 055014 (2013)
[5] P. Bruggeman, G. Cunge, N. Sadeghi. *Plasma Sources Sci. Technol.*, **21**, 035019 (2012)
[6] V. Schulz-von der Gathen, L. Schaper, N. Knake, S. Reuter, K. Niemi, T. Gans, J. Winter. *J. Phys. D: Appl. Phys.*, **41**, 194004 (2008)
[7] K. Niemi, D. O’Connell, N. De Oliveira, D. Joyeux, L. Nahon, J. P. Booth, T. Gans. *Appl. Phys. Lett.*, **103**, 034102 (2013)
[8] L. Nahon, N. de Oliveira, G. Garcia, J. F. Gil, B. Pilette, O. Marcouille, B. Lagarde, F. Polack. *J. Synchrotron Rad.*, **19**, 508 (2012)
[9] N. de Oliveira, M. Roudjane, D. Joyeux, D. Phalippou, J. C. Rodier, L. Nahon. *Nature Photonics*, **5**, 149 (2011)
[10] A. Hibbert, E. Biémont, M. Godefroid, N. Vaeck. *J. Phys. B: At. Mol. Opt. Phys.*, **24**, 3943-3958 (1991)
[11] L. T. Earls. *Phys. Rev.*, **48**, 423-424 (1953)
[12] K. R. German. *J. Chem. Phys.*, **62**, 2584 (1975)
[13] V. L. Kasyutich. *Eur. Phys. J. D*, **33**, 29-33 (2005)
[14] O. A. Alduchov, R. E. Eskridge. *J. Appl. Meteor.*, **35**, 601-609 (1996)
[15] K. Ding, M. A. Lieberman. *J. Phys. D: Appl. Phys.*, **48**, 035401 (2015)
[16] N. Knake, K. Niemi, S. Reuter, V. Schulz-von der Gathen, J. Winter. *Appl. Phys. Lett.*, **93**, 131503 (2008)